

PAPER • OPEN ACCESS

## Investigation of the transfer reactions induced by $^{16}\text{O}$ in $^{27}\text{Al}$ and $^{28}\text{Si}$ at $E_{\text{lab}} = 240 \text{ MeV}$

To cite this article: C. C. Seabra *et al* 2022 *J. Phys.: Conf. Ser.* **2340** 012037

View the [article online](#) for updates and enhancements.

You may also like

- [Effective field theory description of halo nuclei](#)  
H-W Hammer, C Ji and D R Phillips
- [Systematic shell-model study of Rn isotopes with  \$A= 207\$  to 216 and isomeric states](#)  
Bharti Bhoj and Praveen C Srivastava
- [The angular distributions of elastic scattering of  \$^{12,13}\text{C}+\text{Zr}\$](#)   
Cui-Hua Rong, , Gao-Long Zhang et al.

**PRIME**  
PACIFIC RIM MEETING  
ON ELECTROCHEMICAL  
AND SOLID STATE SCIENCE

HONOLULU, HI  
Oct 6–11, 2024

Abstract submission deadline:  
**April 12, 2024**

**Learn more and submit!**

**Joint Meeting of**  
The Electrochemical Society  
•  
The Electrochemical Society of Japan  
•  
Korea Electrochemical Society

# Investigation of the transfer reactions induced by $^{16}\text{O}$ in $^{27}\text{Al}$ and $^{28}\text{Si}$ at $E_{\text{lab}} = 240$ MeV

C. C. Seabra<sup>1\*</sup>, R. Linares<sup>1</sup>, V. A. B. Zagatto<sup>1</sup>, F. Cappuzzello<sup>2,3</sup>, M. Cavallaro<sup>3</sup>, D. Carbone<sup>3</sup>, C. Agodi<sup>3</sup>, J. R. B. Oliveira<sup>4</sup>

<sup>1</sup>Instituto de Física, Universidade Federal Fluminense, 24210-340, Niterói, Rio de Janeiro, Brazil

<sup>2</sup>Istituto Nazionale di Fisica Nucleare, Laboratori Nazionali del Sud, I-95125 Catania, Italy

<sup>3</sup>Dipartimento di Fisica e Astronomia, Università di Catania, I-95125 Catania, Italy

<sup>4</sup>Instituto de Física, Universidade de São Paulo, São Paulo, Brazil

E-mail: \*carolineseabra@id.uff.br

**Abstract.** In this contribution, we present first experimental results for the deuteron pick-up transfer in the  $^{16}\text{O}+^{28}\text{Si}$  system at  $E_{\text{lab.}} = 240$  MeV. This reaction populates states in the  $^{26}\text{Al}$  target-like nucleus. In the same experimental campaign we have also measured the one-proton transfer  $^{28}\text{Si}(^{16}\text{O}, ^{17}\text{F})^{27}\text{Al}$  and one-neutron transfer  $^{27}\text{Al}(^{16}\text{O}, ^{17}\text{O})^{26}\text{Al}$  at the same beam energy. Comparison between the energy spectrum of these transfer reactions indicate that: i) the one-proton and one-neutron transfers favor the population of the low-lying states; ii) deuteron transfer to the ground state in  $^{26}\text{Al}$  is highly suppressed; iii) the cross-sections for deuteron transfer that populates low-lying states in  $^{26}\text{Al}$  are roughly 3 times less than the one-neutron transfer.

## 1. Introduction

Transfer reactions are powerful tools to probe the short range correlations of nucleons inside the nuclear matter [1, 2]. In the past, reactions induced by light ions (p, d, t and  $^3\text{He}$ ) were vastly adopted to study transfers of one and two nucleons. Among these two types, the two-nucleon transfer is of particular interest because it allows to explore the short range correlations in the populated nuclear states. In the two-nucleon transfer, particles can be transferred in two distinct processes: simultaneous and sequential. In the first process, the di-nucleon system acts as single entity and it is transferred in a single step, whereas in the sequential one the two nucleons are independently transferred to an intermediate mass partition upon which the second one is transferred [3, 4].

The large amount of experimental data have shown that transfer reactions are very selective on the population of the nuclear states. Yields can be tuned by appropriate choose of the probe and the incident energy, according to the Brink's rule, that defines the optimal Q-window for transfer reactions [5].

However, the scenario is different with transfers induced by heavy ions. The energy spectra of  $^{14}\text{C}$  nucleus populated by  $^{13}\text{C}(^{18}\text{O}, ^{17}\text{O})$  and  $^{12}\text{C}(^{18}\text{O}, ^{16}\text{O})$  clearly shows that yields of the ground state are suppressed in the two-neutron transfer but well populated in the one-neutron transfer [6]. This means that in heavy systems, the nuclear reaction plays a role in the observed



yields of the nuclear states. Besides, reactions induced by heavy ions allow exploring a large combination of multi-nucleon transfers such as two-neutron (n-n), two-proton (p-p) and deuteron (p-n) transfers. Since the nucleon-nucleon interaction is isospin independent, the dynamics of the two-nucleon transfers shall be similar among the n-n, p-p and deuteron transfers.

Advances on theoretical models and increasing of the computational power have allowed to achieve a good description of transfer reactions induced by heavy ions and to uncover the relative contribution of simultaneous and sequential processes in the two-nucleon transfers [6]. Such theoretical achievement has allowed to explore transfer reaction induced by heavy-ion probes in many target nuclei [7, 8, 9, 10, 11].

Within this context, we are carrying an experimental study of p-, n- and deuteron transfers induced by the  $^{16}\text{O}$  nucleus. The main goal is to probe the short range correlation between proton and neutron in a deuteron transfer in comparison with the two-neutron and two-proton transfers. This proceeding is organized in three different sections: Experimental Setup and data reduction, Experimental results and Conclusions and future perspectives. In this contribution we present first experimental results for the  $^{26}\text{Al}$  nucleus populated by deuteron transfer in the  $^{28}\text{Si}(^{16}\text{O},^{18}\text{F})$  reaction and by the one-neutron transfer in the  $^{27}\text{Al}(^{16}\text{O},^{17}\text{O})$  at  $E_{\text{lab.}}=240$  MeV. We also show the one-proton transfer in the  $^{28}\text{Si}(^{16}\text{O},^{17}\text{F})^{27}\text{Al}$  reaction.

## 2. Experimental Setup and data reduction

The experimental campaign were performed at INFN-LNS, Catania, Italy using the large acceptance MAGNEX spectrometer. In this experiment, a 240 MeV  $^{16}\text{O}$  beam was directed toward  $^{28}\text{Si}$  and  $^{27}\text{Al}$  targets placed in the scattering chamber. The spectrometer's optical axis was set at  $\theta_{\text{lab.}} = 3^\circ$  and,  $8^\circ$  which allow us to cover  $0^\circ - 12^\circ$  angular range. The integrated charged of the incident beam is measured by a Faraday cup placed upstream in the scattering chamber. Projectile-like particles from the target are momentum analyzed by the magnetic elements (quadrupole and dipole) set in full-acceptance mode and detected by a focal plane detector (FPD) placed upstream. The FPD is a hybrid detector consisting of a gaseous part and a set of silicon detectors. The FPD measures parameters associated with the particles' incident trajectory ( $x, y, \theta$  and  $\phi$ ), the energy loss  $\Delta E$  in the gaseous detector and the residual energy  $E_{\text{res.}}$  in the Si detectors. The correlations between these parameters allow a precise isotope identification of the incident particles [12].

A trajectory reconstruction of the detected particles must be applied to obtain the kinematic parameters at the target reference system [13]. This procedure requires an accurate model of the magnetic field distribution inside the quadrupole and dipole that compose the MAGNEX spectrometer. The parameters of the magnetic field model are determined through a systematic comparison between simulated and the experimental data. It is worth to highlight that the elastic and inelastic cross-sections for  $^{16}\text{O} + ^{28}\text{Si}$  and  $^{16}\text{O} + ^{27}\text{Al}$  systems were measured in the same experimental setup [14]. In the simulation, we take into account the kinematics of the reaction in the target, the mean energy loss of the projectile in the target and the spectrometer acceptance.

With the trajectory reconstruction algorithm, we obtain the excitation energy spectrum integrated over an angular range. We were able to achieve an energy resolution of about 0.7 MeV (full width half maximum) and 0.2 MeV energy accuracy. The angular resolution is about  $0.3^\circ$ . Further details on the experimental setup can be found in Refs. [15].

## 3. Experimental results

The excitation energy spectra for the nuclei populated in the reactions studied here are shown in Fig. 1. These spectra are integrated between  $4.0^\circ$  and  $8.0^\circ$  in the laboratory frame. In each energy spectrum, a set of gaussian curves were fitted to the experimental data. The centroid of each gaussian curve corresponds to well known low-lying nuclear states in the projectile-

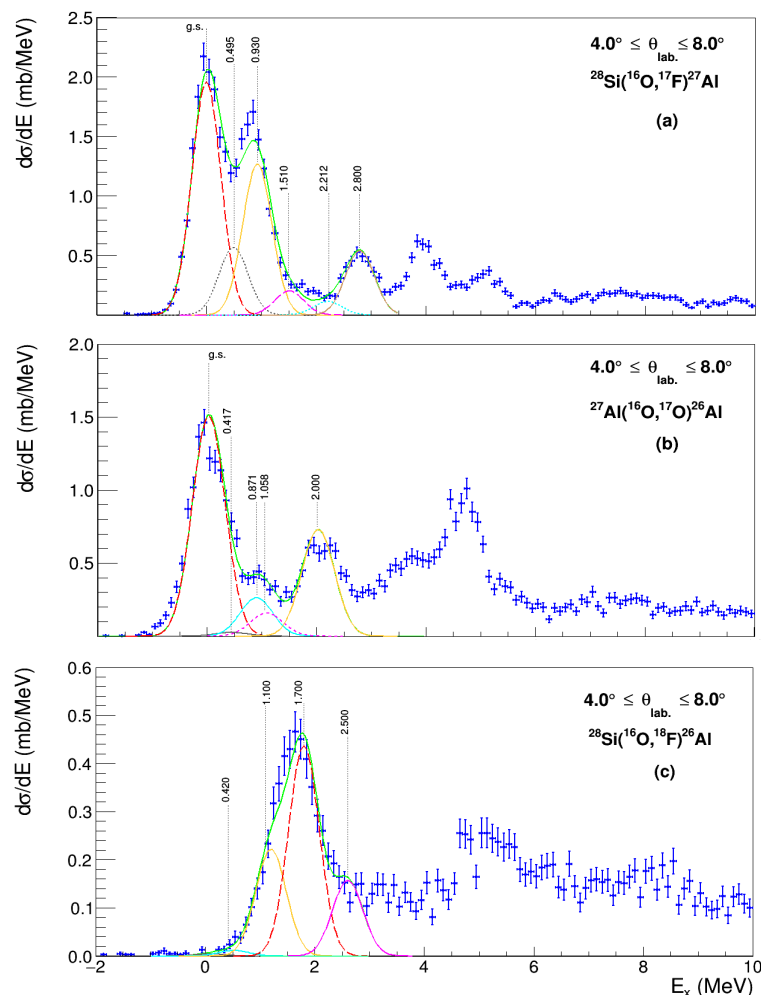


**Figure 1.** Integrated cross-section as a function of excitation energy for the p-transfer in  $^{28}\text{Si}$  (panel a), the n-transfer in  $^{27}\text{Al}$  (panel b) and the d-transfer in  $^{28}\text{Si}$  (panel c) reactions, respectively. Energy spectra are reproduced by adjusted gaussian curves that reproduce nuclear states. See text for more details.

and target-like nuclei, while the width of all gaussian curves was set fixed to represent the experimental energy resolution. The amplitude of the gaussian curves was set as an adjustable parameter of the fitting model. In some cases, a gaussian curve represents a group of nuclear states whose relative energies are well below the achieved energy resolution. Additionally, the green solid curves in each energy spectrum correspond to the sum of these individual gaussian curves and describe reasonably well our data points.

For the  $^{28}\text{Si}(^{16}\text{O},^{17}\text{F})^{27}\text{Al}$  reaction, the energy spectrum (Fig. 1a) shows that the low-lying states are well populated. This is also the case in the  $^{27}\text{Al}(^{16}\text{O},^{17}\text{O})^{26}\text{Al}$  reaction (Fig. 1b). In both spectra, the dashed red curve represents the ground state of  $^{17}\text{F} + ^{27}\text{Al}$  (in the case of p-transfer) and  $^{17}\text{O} + ^{26}\text{Al}$  (in the case of n-transfer). Comparison between the excitation energy spectra for both p-transfer and n-transfer shows that ground-to-ground one-nucleon transfers

1.100 MeV peak		1.700 MeV peak		2.500 MeV peak	
$^{26}\text{Al}$ states	$^{18}\text{F}$ states	$^{26}\text{Al}$ states	$^{18}\text{F}$ states	$^{26}\text{Al}$ states	$^{18}\text{F}$ states
1.058	1.042	1.759	1.701	2.365	2.523
-	1.081	1.851	-	2.545	-
-	1.121	-	-	-	-

**Table 1.** List of nuclear states in  $^{18}\text{F}$  and  $^{26}\text{Al}$  states observed in d-pickup reaction with the  $^{28}\text{Si}$  target. The peaks 1.100 MeV, 1.700 MeV and 2.500 MeV are represented by solid yellow, dashed red and solid magenta curves in Fig. 1c.

are predominant. The integrated cross-section for the ground state in the  $^{28}\text{Si}(^{16}\text{O}, ^{17}\text{F})^{27}\text{Al}$  is 1.46(15) mb and in the  $^{27}\text{Al}(^{16}\text{O}, ^{17}\text{O})^{26}\text{Al}$  reaction is 1.03(10) mb.

Based on our fitting model, the population of the first excited state, namely the first excited state in  $^{17}\text{F}$  at 0.495 MeV and the second excited state in  $^{26}\text{Al}$  at 0.417 MeV are weakly populated (dotted gray line in Fig. 1a). The first two excited states in  $^{27}\text{Al}$  (0.844 and 1.015 MeV) are represented by a single gaussian curve centered at 0.930 MeV (solid yellow line). The peak at 1.510 MeV represents the sum of  $^{17}\text{F}$  and  $^{27}\text{Al}$ , both in their first excited state (dashed magenta line). The peak at 2.212 MeV represents the third excited state in  $^{27}\text{Al}$  (solid cyan line). Finally, the peak at 2.800 MeV represents the contribution of higher excited states of  $^{27}\text{Al}$  (solid maroon line). For the  $^{27}\text{Al}(^{16}\text{O}, ^{17}\text{O})^{26}\text{Al}$  reaction, we have considered the contribution of the second excited state of  $^{26}\text{Al}$  at 0.417 MeV (solid gray line in Fig. 1b) followed by  $^{17}\text{O}$  first excited state at 0.871 MeV (solid cyan line) and  $^{26}\text{Al}$  third excited state at 1.058 MeV (dashed magenta line). The last peak, at about 2.000 MeV, represents a set of three  $^{26}\text{Al}$  states at 2.068 MeV, 2.069 MeV and 2.071 MeV (solid yellow line), which cannot be individually fitted due to the resolution of the experiment.

Fig. 1(c) shows the energy spectrum for the deuteron transfer reaction in the  $^{28}\text{Si}$  target. It must be highlighted that the same target-like nucleus ( $^{26}\text{Al}$ ) is also populated in the  $^{27}\text{Al}(^{16}\text{O}, ^{17}\text{O})^{26}\text{Al}$  reaction (Fig 1b), even though the energy spectra observed in these two reactions are clearly different. The ground state in  $^{18}\text{F}+^{26}\text{Al}$  system is highly suppressed, with an estimated integrated cross-section of 3  $\mu\text{b}$ . The cross-section for deuteron transfer leading to the second excited state of  $^{26}\text{Al}$  (solid cyan line in Fig. 1c) also shows a quite low value, of about 8  $\mu\text{b}$ . Accurate values for these cross-sections requires a proper treatment of the shape of the background. Nevertheless, it is clear that the d-transfer does not favor the population of the ground states of  $^{18}\text{F}$  and  $^{26}\text{Al}$ . This reaction populates predominantly states around 1.1 MeV (solid yellow line) and 1.7 MeV (dashed red line). These energies represent a combination of some excited states in  $^{18}\text{F}$  and  $^{26}\text{Al}$  (see Table 1) and the cross-sections are 0.16(5) mb and 0.30(5) mb, respectively. This is about 3 times less than the values for one-neutron transfer leading to the ground state in  $^{26}\text{Al}$ .

#### 4. Conclusion and future perspectives

In this contribution we present the first experimental results for  $^{28}\text{Si}(^{16}\text{O}, ^{17}\text{F})^{27}\text{Al}$ ,  $^{27}\text{Al}(^{16}\text{O}, ^{17}\text{O})^{26}\text{Al}$  and  $^{28}\text{Si}(^{16}\text{O}, ^{18}\text{F})^{26}\text{Al}$  reactions. These reactions were measured in the same experimental campaign at INFN-LNS using the large acceptance MAGNEX spectrometer. The same procedure for data reduction was carried out to minimize systematic uncertainties that may rise from the trajectory reconstruction algorithm. The excitation energy spectra obtained for each reaction show that the ground state and first excited states are strongly suppressed in the deuteron transfer on the  $^{28}\text{Si}$  target, selectively populating a few states of  $^{26}\text{Al}$  and  $^{18}\text{F}$ . Also, the experimental cross-sections for deuteron transfer is about 3 times less than the neutron

transfer induced on  $^{27}\text{Al}$  leading to the same residual nucleus.

In the next steps, we will finish the data reduction and cross-section extraction for a complementary dataset measured at  $3^\circ$ . This allows us to independently check the consistency of our results and to obtain cross-sections around  $0^\circ$ . Moreover, from the same dataset, we will extract cross-sections for the two- and one-proton transfers on the  $^{28}\text{Si}$  target and one-proton transfer on  $^{27}\text{Al}$  target.

## Acknowledgments

The first author would like to acknowledge for the financial support from the IAEA Marie Skłodowska-Curie Fellowship Programme. The Brazilian authors acknowledge partial financial support from CNPq, FAPERJ and from INCT-FNA (Instituto Nacional de Ciência e Tecnologia - Física Nuclear e Aplicações), research project 464898/2014-5.

## 5. References

- [1] Kahana S and Baltz A 1977 *Advances in Nuclear Physics* (Springer) pp 1–122
- [2] Wu C, Oertzen W, Cline D and Guidry M 1990 *Annual Review of Nuclear and Particle Science* **40** 285–326
- [3] Mermaz M C, Whitten C A, Champlin J W, Howard A J and Bromley D A 1971 *Phys. Rev. C* **4**(5) 1778–1800
- [4] Bohne W, Fuchs H, Grabisch K, Hagen M, Homeyer H, Janetzki U, Lettau H, Maier K, Morgenstern H, Pietrzyk P *et al.* 1969 *Nuclear Physics A* **131** 273–304
- [5] Brink D 1972 *Physics Letters B* **40** 37 – 40 ISSN 0370-2693
- [6] Cavallaro M, Cappuzzello F, Bondi M, Carbone D, Garcia V N, Gargano A, Lenzi S M, Lubian J, Agodi C, Azaiez F, De Napoli M, Foti A, Franchoo S, Linares R, Nicolosi D, Niikura M, Scarpaci J A and Tropea S 2013 *Phys. Rev. C* **88**(5) 054601
- [7] Carbone D, Ferreira J L, Cappuzzello F, Lubian J, Agodi C, Cavallaro M, Foti A, Gargano A, Lenzi S M, Linares R and Santagati G 2017 *Phys. Rev. C* **95**(3) 034603
- [8] Linares R, Ermamatov M J, Lubian J, Cappuzzello F, Carbone D, Cardozo E N, Cavallaro M, Ferreira J L, Foti A, Gargano A, Paes B, Santagati G and Zagatto V A B 2018 *Phys. Rev. C* **98**(5) 054615
- [9] Carbone D, Ferreira J L, Calabrese S, Cappuzzello F, Cavallaro M, Hacisalihoglu A, Lenske H, Lubian J, Magaña Vsevolodovna R I, Santopinto E, Agodi C, Acosta L, Bonanno D, Borello-Lewin T, Boztosun I, Brischetto G A, Burrello S, Calvo D, Chávez Lomelí E R, Ciraldo I, Colonna M, Delaunay F, Deshmukh N, Finocchiaro P, Fisichella M, Foti A, Gallo G, Iazzi F, La Fauci L, Lanzalone G, Linares R, Medina N H, Morales M, Oliveira J R B, Pakou A, Pandola L, Petrascu H, Pinna F, Russo G, Sgouros O, Solakci S O, Soukeras V, Souliotis G, Spatafora A, Torresi D, Tudisco S, Yildirim A and Zagatto V A B (NUMEN Collaboration) 2020 *Phys. Rev. C* **102**(4) 044606
- [10] Calabrese S, Cavallaro M, Carbone D, Cappuzzello F, Agodi C, Burrello S, De Gregorio G, Ferreira J L, Gargano A, Sgouros O, Acosta L, Amador-Valenzuela P, Bellone J I, Borello-Lewin T, Brischetto G A, Calvo D, Capirossi V, Chávez Lomelí E R, Ciraldo I, Colonna M, Delaunay F, Djapo H, Eke C, Finocchiaro P, Firat S, Fisichella M, Foti A, Guazzelli M A, Hacisalihoglu A, Iazzi F, La Fauci L, Lay J A, Linares R, Lubian J, Medina N H, Morales M, Oliveira J R B, Pakou A, Pandola L, Petrascu H, Pinna F, Russo G, Solakci S O, Soukeras V, Souliotis G, Spatafora A, Torresi D, Tudisco S, Yildirim A and Zagatto V A B (NUMEN Collaboration) 2021 *Phys. Rev. C* **104**(6) 064609
- [11] Sgouros O, Cavallaro M, Cappuzzello F, Carbone D, Agodi C, Gargano A, De Gregorio G, Altana C, Brischetto G A, Burrello S, Calabrese S, Calvo D, Capirossi V, Chávez Lomelí E R, Ciraldo I, Cutuli M, Delaunay F, Djapo H, Eke C, Finocchiaro P, Fisichella M, Foti A, Hacisalihoglu A, Iazzi F, La Fauci L, Linares R, Lubian J, Medina N H, Morales M, Oliveira J R B, Pakou A, Pandola L, Pinna F, Russo G, Guazzelli M A, Soukeras V, Souliotis G, Spatafora A, Torresi D, Yildirim A and Zagatto V A B (for the NUMEN Collaboration) 2021 *Phys. Rev. C* **104**(3) 034617
- [12] Cappuzzello F, Cavallaro M, Cunsolo A, Foti A, Carbone D, Orrigo S and Rodrigues M 2010 *Nuclear Instruments and Methods in Physics Research Section A: Accelerators, Spectrometers, Detectors and Associated Equipment* **621** 419–423
- [13] Cappuzzello F, Carbone D and Cavallaro M 2011 *Nuclear Instruments and Methods in Physics Research Section A: Accelerators, Spectrometers, Detectors and Associated Equipment* **638** 74–82 ISSN 0168-9002
- [14] Fonseca L M, Linares R, Zagatto V A B, Cappuzzello F, Carbone D, Cavallaro M, Agodi C, Lubian J and Oliveira J R B 2019 *Phys. Rev. C* **100**(1) 014604
- [15] Cappuzzello F, Agodi C, Carbone D and Cavallaro M 2016 *The European Physical Journal A* **52** 1–44